SIAM J. APPL. MATH.
Vol. 64, No. 2, pp. 546–564

ON THE NATURE OF INITIAL-BOUNDARY VALUE SOLUTIONS FOR DISPERSIVE EQUATIONS*

NATASHA FLYER† AND BENGT FORNBERG‡

Abstract. If the initial and boundary data for a partial differential equation (PDE) do not obey an infinite set of compatibility conditions, singularities will arise in its solutions. For dissipative equations, these singularities are well localized in both time and space, and an effective numerical remedy is available for accurate computation of initial transients. This study analyzes the nature of similar corner discrepancies for dispersive equations, such as $u_t - u_{xxx} = 0$ and $iu_t - u_{xx} = 0$.

Key words. time-space corner singularities, dispersive equations, initial-boundary value problems

AMS subject classifications. 35B05, 35B30, 35B65, 35A20

DOI. 10.1137/S0036139902415853

1. Introduction.

Solutions to initial-boundary value problems (IBVPs) will feature "corner singularities" in the space-time domain where initial and boundary data meet, unless these two data sets are connected by an infinite number of compatibility conditions [2]. Since the two data sets usually arise from different considerations, these singularities are almost always present. Although the issue has been analyzed at least since the 1950s (as surveyed in [2] and [3]), the focus has mostly been theoretical rather than numerical. For dissipative equations, the irregularities that are caused by these corner singularities are short-lived in time and remain local in space. These features allowed for the development of a highly effective strategy for restoring full numerical accuracy with little extra computational cost, as described in [4]. For dispersive PDEs, the irregularities do not stay local in space, and it depends on the equation whether or not they will be short-lived in time. Methods for effective numerical treatment will likely vary from equation to equation. The goal of the present paper is to give illustrating examples of dispersive corner singularities, largely by means of finding corner basis functions, which illuminate the mixing of temporal and/or spatial scales that occurs initially. If the boundaries are introduced to the problem only for the purpose of truncating what otherwise would have been an infinite domain, the preferred strategy would quite certainly be to create artificial boundary conditions in such a way that these space-time domain corner singularities do not arise.

Section 2 introduces the concept of corner basis functions, first for the well-known model equations $u_t + u_x = 0$ and $u_t - u_{xx} = 0$. It is shown how corner basis functions describe the nature of the corner singularities for these equations. Since the general character of solutions to dispersive equations may be less familiar, section 3 starts with some illustrative solutions for the linearized KdV equation, $u_t - u_{xxx} = 0$, and then proceeds with establishing its corner basis functions. Section 4 contains a similar discussion for the linear Schrödinger equation, $iu_t - u_{xx} = 0$. Based on these corner basis functions, we discuss in section 5 the character of IBV solutions for the two

*Received by the editors October 4, 2002; accepted for publication (in revised form) June 3, 2003; published electronically December 31, 2003. This work was supported by NSF grants DMS-9810751 (VIGRE), DMS-0073048, and DMS-0309803.
http://www.siam.org/journals/siap/64-2/41585.html
†National Center for Atmospheric Research, P.O. Box 3000, Boulder, CO 80305 (flyer@ucar.edu).
‡University of Colorado, Department of Applied Mathematics, 526 UCB, Boulder, CO 80309 (fornberg@colorado.edu).

dispersive equations just mentioned. The final section offers some concluding remarks, summarizing the nature of corner singularities for PDEs of the type $u_t \pm u_{nx} = 0$, $n = 1, 2, 3, \ldots$, in terms of corner basis functions.

2. Corner basis functions for $u_t + u_x = 0$ and $u_t - u_{xx} = 0$. The quarter plane problem ($x > 0,\ t > 0$)

$$\begin{aligned} &\text{PDE:} && u_t + u_x = 0, \\ &\text{IC:} && u(x,0) = f(x), \\ &\text{BC:} && u(0,t) = g(t) \end{aligned} \tag{2.1}$$

has the analytic solution

$$u(x,t) = \begin{cases} f(x-t), & x > t, \\ g(t-x), & x < t. \end{cases} \tag{2.2}$$

Assuming that $f(x)$ and $g(t)$ are smooth functions, the solution (2.2) is smooth for all times if and only if an infinite sequence of compatibility conditions holds in the corner at $x = 0$, $t = 0$ [2], [3]:

$$\begin{aligned} &g(0) - f(0) && = 0, && \text{continuity} \\ &g_t(0) + f_x(0) && = 0, && \text{PDE} \\ &g_{tt}(0) - f_{xx}(0) && = 0, && \text{differentiated versions of the PDE} \\ &g_{ttt}(0) + f_{xxx}(0) && = 0, && \quad\downarrow \\ &\vdots \\ &g_{nt}(0) + (-1)^{n+1} f_{nt}(0) && = 0. \end{aligned} \tag{2.3}$$

If we are given a problem (2.1) for which any of the equalities in (2.3) fail to hold, one strategy for transforming the problem to one with a smooth solution (better suited for most numerical methods) is to create an explicitly known function $s(x,t)$ which also satisfies the PDE and which possesses an identical corner singularity. To construct $s(x,t)$, we introduce the concept of corner basis functions $u_n(x,t)$ with the properties

(2.4) (i) $u_n(x,t)$ satisfies the PDE away from the corner,

(ii) $u_n(x,0) \equiv 0$,

(iii) $$\frac{1}{n!}\frac{\partial^j u_n(0,t)}{\partial t^j} = \begin{cases} 1 & \text{for } j = k, \\ 0 & \text{for } j \neq k. \end{cases}$$

The corner basis functions are derived by Taylor expanding the boundary condition (BC) in time and then for each term in the expansion solving the PDE with zero initial condition (IC), as shown below in the case of (2.1).

$$\begin{aligned} u_0(x,t) &= \begin{cases} 0, & x > t, \\ 1, & x < t, \end{cases} \\ u_1(x,t) &= \begin{cases} 0, & x > t, \\ t - x, & x < t, \end{cases} \\ u_2(x,t) &= \begin{cases} 0, & x > t, \\ (t-x)^2, & x < t, \end{cases} \\ &\cdots, \end{aligned} \tag{2.5}$$

i.e.,

$$u_n(x,t) = \begin{cases} 0, & x > t, \\ (t-x)^n, & x < t, \end{cases} \quad n = 0, 1, 2, \dots .$$

If the right-hand sides of (2.3) were not equal to 0, 0, 0, 0, ... but instead equal to $r_0,\ r_1,\ r_2,\ r_3,\ \dots$, the function

$$s(x,t) = r_0\, u_0(x,t) + \frac{r_1}{1!}\, u_1(x,t) + \frac{r_2}{2!}\, u_2(x,t) + \frac{r_3}{3!}\, u_3(x,t) + \cdots \tag{2.6}$$

would have exactly the same corner singularity as the solution $u(x,t)$. Standard numerical methods can then be applied to the difference function

$$v(x,t) = u(x,t) - s(x,t), \tag{2.7}$$

which is infinitely smooth and well suited for numerics (satisfying the same PDE and IC, and having known BCs). However, in practice, we are limited to machine precision and thus need to use only a finite number p of compatibility conditions, corresponding to a truncated version of (2.6). The difference in (2.7) will be of size $O(t^p)$, the first neglected term in the expansion $s(x,t)$. For small t, we can make this difference arbitrarily small by choosing p sufficiently large.

This idea of creating corner singularity functions $u_n(x,t),\ n = 0, 1, 2, \dots$, and then subtracting a combination of them is of no particular utility for (2.1) since the analytic solution (2.2) is almost as simple algebraically as are the corner functions (2.5). Furthermore, the corner irregularity will persist for all times. If (2.1) is generalized to variable coefficients, the singularity will travel along a curved characteristic path, and cancellation based solely on corner information is not feasible.

Turning to the heat equation, it may at first appear that corner corrections are not needed. Figures 2.1(a), (b) show the analytic solution to the IBVP

$$\begin{aligned} &\text{PDE:} \quad u_t - u_{xx} = 0, \\ &\text{IC:} \quad\ u(x,0) \quad = 0, && 0 \le x \le 1, \\ &\text{BCs:} \begin{cases} u(0,t) & = \sin 2\pi t, \\ u_x(1,t) & = 0, \end{cases} && t > 0, \end{aligned} \tag{2.8}$$

over $0 \le x \le 1,\ 0 \le t \le 1$ and $0 \le x \le 10^{-3},\ 0 \le t \le 10^{-3}$, respectively. No matter how much we zoom in on the area near the origin, the solution surface will graphically look indistinguishable from the one shown to the right (Figure 2.1(b)).

However, this apparent regularity of the solution near the origin is severely misleading. The seemingly smooth solution in fact features a sharp irregularity, as the plot over $0 \le x \le 1,\ 0 \le t \le 10^{-3}$ in Figure 2.2(a) reveals.

A 21-node numerical Chebyshev solution (implemented without grid clustering at the right boundary, cf. [6, section 5.1, Example 3], and using a fourth-order Runge–Kutta method in time) will feature errors of the order 10^{-4} near the origin during the first moments, due to the fact that the PDE is not satisfied in the corner $(0,0)$ by the solution. This numerical observation is theoretically proven in [3]. At later times, the error decreases to around 10^{-12}. In Figure 2.2(b), the numerical corner error has already decayed to around 10^{-6} by the first displayed time level.

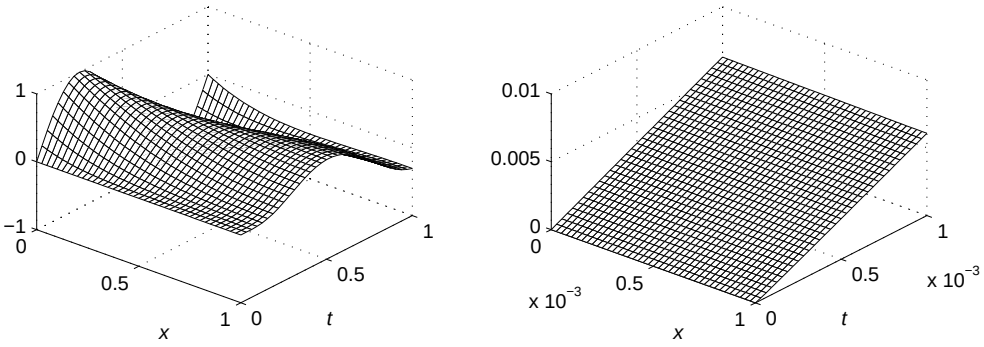

FIG. 2.1. *Analytic solution to the IBV problem* (2.8) *shown over* (a) $0 \le x \le 1,\ 0 \le t \le 1$ *and* (b) $0 \le x \le 10^{-3},\ 0 \le t \le 10^{-3}$.

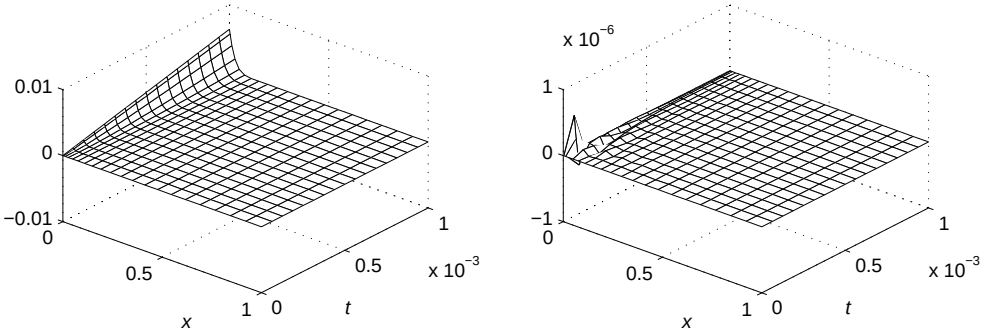

FIG. 2.2. (a) *Analytic solution to IBV problem* (2.8). (b) *Error in Chebyshev numerical solution. Both are shown over* $0 \le x \le 1,\ 0 \le t \le 10^{-3}$ *and displayed on a grid that is quadratically refined at the left edge.*

Although corner irregularities for the heat equation persist only a very short time, corrections for them are needed in order to obtain an accurate solution of initial transients. For the constant coefficient case

$$\begin{aligned} &\text{PDE:} && u_t - u_{xx} = 0, && \\ &\text{IC:} && u(x,0) = f(x), && x > 0, \\ &\text{BC:} && u(0,t) = g(t), && t > 0, \end{aligned} \tag{2.9}$$

we need to replace the compatibility conditions (2.3) by

$$\begin{aligned} g(0) - f(0) &= 0, && \text{continuity} \\ g_t(0) - f_{xx}(0) &= 0, && \text{PDE} \\ g_{tt}(0) - f_{xxxx}(0) &= 0, && \text{differentiated versions of the PDE} \\ \dots, & && \downarrow \\ g_{nt}(0) - f_{(2n)x}(0) &= 0, && \end{aligned}$$

and the corner functions (2.5) by

$$
\begin{aligned}
u_0(x,t) &= \operatorname{Erfc}\left(\tfrac{x}{2\sqrt{t}}\right),\\
u_1(x,t) &= -\sqrt{\tfrac{t}{\pi}}\; x\; e^{-x^2/(4t)} + \left(t+\tfrac{x^2}{2}\right)\operatorname{Erfc}\left(\tfrac{x}{2\sqrt{t}}\right),\\
u_2(x,t) &= -\tfrac{1}{6}\sqrt{\tfrac{t}{\pi}}\; x\; (10\,t+x^2)\; e^{-x^2/(4t)} + \left(t^2+t\,x^2+\tfrac{x^4}{12}\right)\operatorname{Erfc}\left(\tfrac{x}{2\sqrt{t}}\right),\\
u_3(x,t) &= -\tfrac{1}{60}\sqrt{\tfrac{t}{\pi}}\; x\; (132\,t^2+28\,t\,x^2+x^4)\; e^{-x^2/(4t)}\\
&\quad + \left(t^3+\tfrac{3}{2}t^2x^2+\tfrac{1}{4}t\,x^4+\tfrac{x^6}{120}\right)\operatorname{Erfc}\left(\tfrac{x}{2\sqrt{t}}\right),\\
&\ldots .
\end{aligned}
\tag{2.10}
$$

These functions all satisfy the PDE with the IC and BC $u_n(x,0)=0,\ u_n(0,t)=t^n,\ n=0,1,2,\ldots$.

One way to derive (2.10) is to note that the change of variables $\xi=\frac{x}{\sqrt{t}},\ \tau=\log t$ transforms $u_t-u_{xx}=0$ into $u_\tau=u_{\xi\xi}+\frac{\xi}{2}u_\xi$. The $u_0(x,t)$ solution corresponds to an equilibrium solution of the transformed PDE. With the BCs $u(0)=1,\ u(\infty)=0$ we find $u(\xi)=\operatorname{Erfc}(\frac{\xi}{2})$ $(=1-\frac{2}{\sqrt{\pi}}\int_0^{\xi/2}e^{-\varsigma^2}d\varsigma)$, and consequently $u_0(x,t)=\operatorname{Erfc}(\frac{x}{2\sqrt{t}})$. The subsequent corner functions can then (like for all other PDEs) be generated recursively:

$$
u_n(x,t) = n\int_0^t u_{n-1}(x,t)\,dt, \quad n=1,2,\ldots . \tag{2.11}
$$

Alternatively, we can obtain a general expression for all the $u_n(x,t)$ functions in terms of Kummer's confluent ${}_1F_1$ hypergeometric functions:

$$
u_n(x,t) = t^n\left\{{}_1F_1(-n,\tfrac{1}{2},-\tfrac{x^2}{4t}) - \tfrac{x\,\Gamma(n+1)}{\sqrt{t}\,\Gamma(n+\frac{1}{2})}\;{}_1F_1(\tfrac{1}{2}-n,\tfrac{3}{2},-\tfrac{x^2}{4t})\right\},\ n=0,1,2,\ldots . \tag{2.12}
$$

To arrive at (2.12), we generalize the observation above regarding the $u_0(x,t)$ corner function by noting that $\frac{u_n(x,t)}{t^n}$ becomes a function of one variable $\xi=\frac{x}{\sqrt{t}}$ only, which we write as $u_n(\xi)$. From its definition and the governing PDE, this function will need to satisfy

$$
(u_n)_{\xi\xi}+\frac{\xi}{2}(u_n)_\xi - n\,u_n = 0 \quad \text{with} \quad \begin{cases} u_n(0) &= 1,\\ u_n(\infty) &= 0. \end{cases}
$$

The general solution to the ODE can be written

$$
u_n(\xi) = c_1\;\; {}_1F_1(-n,\tfrac{1}{2},-\tfrac{\xi^2}{4}) + c_2\;\xi\;\; {}_1F_1(\tfrac{1}{2}-n,\tfrac{3}{2},-\tfrac{\xi^2}{4}).
$$

The condition $u_n(0)=1$ says that $c_1=1$, and leading order asymptotics of the ${}_1F_1$ functions (see [1]) demonstrate that cancellation of growths as $\xi\to\infty$ requires $\frac{c_2}{c_1}=-\frac{\Gamma(n+1)}{\Gamma(n+\frac{1}{2})}$.

Figure 2.3 shows $u_0(x,t),\ u_1(x,t)$, and $u_2(x,t)$ displayed over two different time intervals. The irregularity remains local in both time and space. For dissipative equations like (2.9), corner functions form a very effective means of improving the accuracy of numerical calculations since, as is shown in [4],

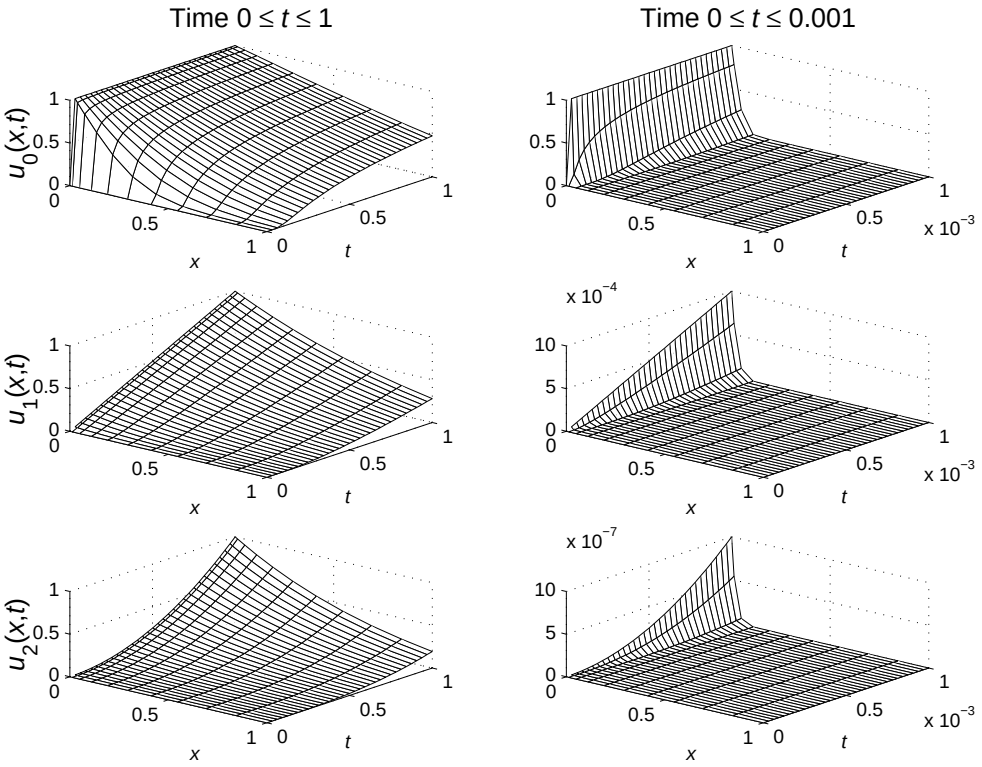

FIG. 2.3. *The corner functions* $u_0(x,t)$, $u_1(x,t)$, *and* $u_2(x,t)$ *for the heat equation* $u_t - u_{xx} = 0$, *shown over* $0 \le x \le 1$ *and (left column)* $0 \le t \le 1$, *(right column)* $0 \le t \le 0.001$. *The grid is again quadratically refined towards the left edge.*

1. only 3–4 correction functions typically suffice for correction to machine precision, and
2. generalizations to variable coefficients are straightforward.

3. Illustrative solutions and corner functions for $u_t - u_{xxx} = 0$. Similar to the heat equation, IBV solutions to the linearized KdV equation

$$u_t - u_{xxx} = 0 \tag{3.1}$$

will typically feature two scales: (1) a slow, long-term part and (2) a high-frequency part emanating from the corners and described by corner basis functions. Initially, the high-frequency part of the solution is of infinitesimal size but then expands to cover the whole domain. To illustrate the first part and to provide a background for discussing the latter part, we first consider different half-plane problems containing only slow long-term scales.

3.1. Traveling wave solutions in different half-planes.

3.1.1. The upper half-plane ($t > 0$). With the IC

$$\text{IC:} \quad u(x,0) = \cos(kx), \tag{3.2}$$

the solution of (3.1) becomes

$$\text{solution:} \quad u(x,t) = \cos(kx - k^3 t). \tag{3.3}$$

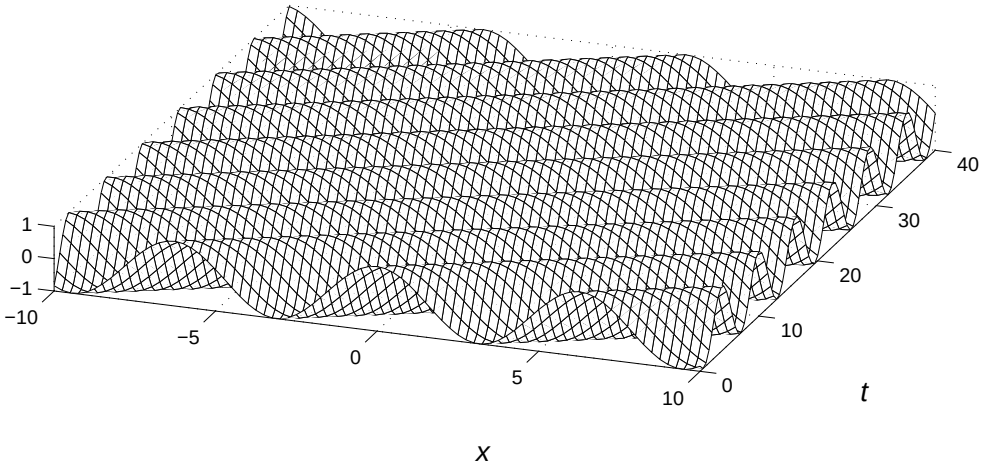

FIG. 3.1. *Upper half-plane solution to* $u_t - u_{xxx} = 0$ *with IC* $u(x,0) = \cos(x)$.

This is a single Fourier mode whose phase speed increases with the wave number k as $c = k^2$. We can note that *all* waves travel to the right, as shown in Figure 3.1 for $k = 1$.

3.1.2. The right half-plane ($x > 0$). For the equation (3.1) we need to impose two BCs on the left side (taken to be $x = 0$). Two cases can be noted. The first case has a sinusoidal forcing on the boundary, with the first derivative $u_x(0,t) = 0$.

Case 1.

$$\text{BCs:} \quad \begin{cases} u(0,t) = \sin(k^3 t), \\ u_x(0,t) = 0, \end{cases}$$

$$\text{solution:} \quad u(x,t) = \tfrac{1}{\sqrt{3}} \left[\cos(kx - k^3 t + \tfrac{\pi}{3}) - e^{-\frac{\sqrt{3}}{2}kx} \cos(\tfrac{1}{2}kx + k^3 t + \tfrac{\pi}{3}) \right].$$

In the second case, the solution is zero and it is the first derivative that has a sinusoidal forcing:

Case 2.

$$\text{BCs:} \quad \begin{cases} u(0,t) = 0, \\ u_x(0,t) = \sin(k^3 t), \end{cases}$$

$$\text{solution:} \quad u(x,t) = \tfrac{1}{\sqrt{3}\,k} \left[\cos(kx - k^3 t + \tfrac{\pi}{6}) - e^{-\frac{\sqrt{3}}{2}kx} \cos(\tfrac{1}{2}kx + k^3 t - \tfrac{\pi}{6}) \right].$$

Figures 3.2 and 3.3 show Cases 1 and 2, respectively. We notice in Figure 3.2 how the crests of the waves emerge perpendicularly to the left boundary in order to accommodate the zero first derivative BC. Similarly, Figure 3.3 shows how the waves again are deformed near the boundary, this time to accommodate the condition $u(0,t) = 0$. As these two cases demonstrate, forcing the left boundary with a Fourier mode will produce outgoing waves with the same wave number, differing between the two cases only in amplitude and phase shift. It is therefore possible to create a

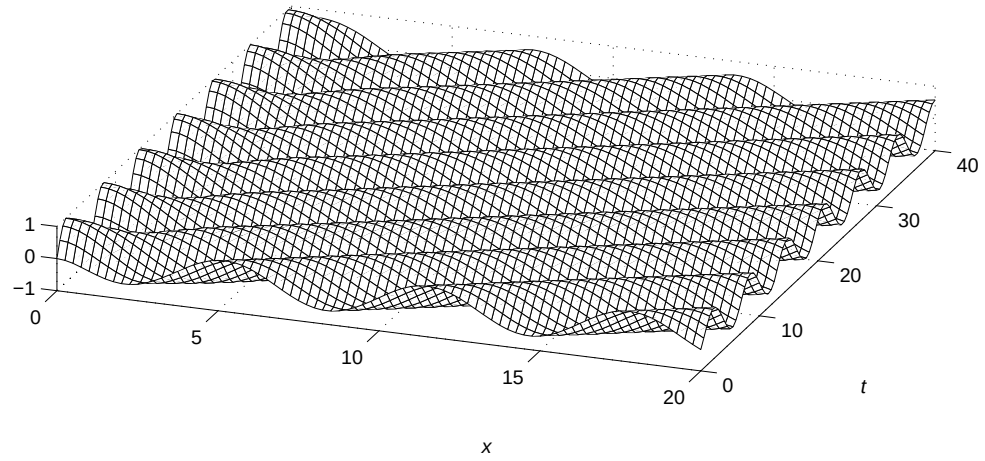

FIG. 3.2. *Solution to the right half-plane problem for* $u_t - u_{xxx} = 0$ *with the left BCs* $u(0,t) = \sin t,\ u_x(0,t) = 0$.

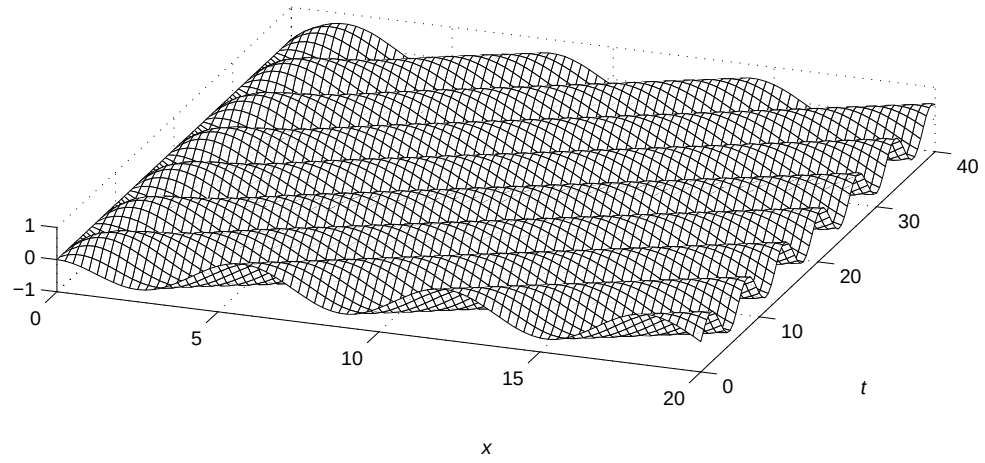

FIG. 3.3. *Solution to the right half-plane problem for* $u_t - u_{xxx} = 0$ *with left BCs* $u(0,t) = 0,\ u_x(0,t) = \sin t$.

BC so that the outgoing waves cancel, and only the exponential decay to the right remains. However, this is a very special case; sinusoidal forcing will in general produce sinusoidal waves traveling to the right.

3.1.3. The left half-plane ($x < 0$). For the right half-plane problems, we considered forcing on the left side. We now consider forcing on the right side, requiring only one BC for the PDE:

$$\begin{aligned} &\text{BC:} && u(0,t) = \sin(k^3 t), \\ &\text{solution:} && u(x,t) = e^{\frac{\sqrt{3}}{2}kx} \sin(\tfrac{1}{2}kx + k^3 t). \end{aligned}$$

There can be no waves traveling to the left for (3.1), and the solution therefore decays exponentially away from the boundary, as is seen in Figure 3.4. This also implies that

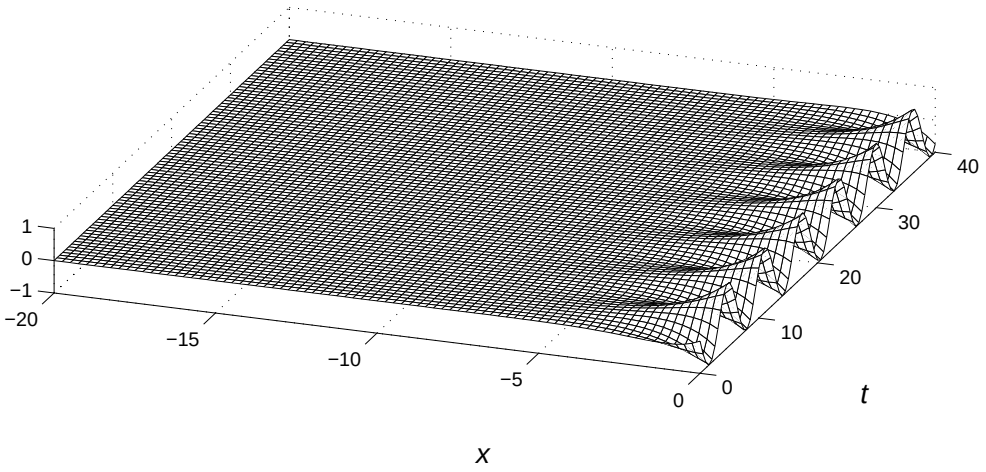

FIG. 3.4. *Solution to the left half-plane problem for* $u_t - u_{xxx} = 0$ *with forcing* $u(0,t) = \sin t$ *on the right boundary.*

when waves arrive from the left to a right boundary, there can be no reflection, but only decay. With incoming waves of the form $u(x,t) = \cos(kx - k^3 t)$, closed form solutions for the cases with Neumann and Dirichlet right BCs become as follows.

Case 1.

$$\begin{aligned} &\text{BC:} && u_x(0,t) = 0, \\ &\text{solution:} && u(x,t) = \cos(kx - k^3 t) + e^{\frac{\sqrt{3}}{2}kx} \cos(\tfrac{1}{2}kx + k^3 t + \tfrac{\pi}{3}). \end{aligned}$$

Case 2.

$$\begin{aligned} &\text{BC:} && u(0,t) = 0, \\ &\text{solution:} && u(x,t) = \cos(kx - k^3 t) - e^{\frac{\sqrt{3}}{2}kx} \cos(\tfrac{1}{2}kx + k^3 t). \end{aligned}$$

These solutions are shown in Figures 3.5 and 3.6.

In both cases, the incoming wave from the left undergoes a transition near the right boundary in order to accommodate the BCs at the right edge. The half-plane solutions for (3.1) can be summed up as waves traveling *solely* to the right, with at most a thin transition region at a right-hand boundary. The character of these half-plane solutions set the stage for solving the quarter-plane problem, leading us to sets of left and right corner basis functions.

3.2. Left corner functions. Since (3.1) needs two BCs to the left, we need to obtain two independent sets of corner functions $u_n(x,t)$ and $v_n(x,t)$. These functions should all obey the PDE, the IC $u_n(x,0) = v_n(x,0) = 0$, and the BCs

$$\begin{cases} u_n(0,t) = t^n, & \frac{\partial}{\partial x} u_n(0,t) = 0, \\ v_n(0,t) = 0, & \frac{\partial}{\partial x} v_n(0,t) = t^n, \end{cases} \qquad n = 0,\ 1,\ 2,\ \ldots .$$

Following the approach which led us to the corner functions (2.12) for the heat

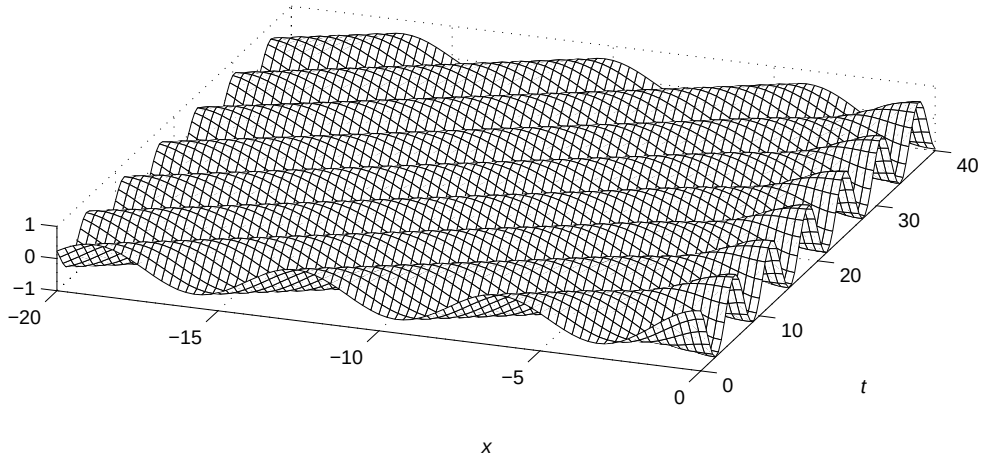

FIG. 3.5. *Solution to the left half-plane problem for* $u_t - u_{xxx} = 0$ *with incoming sinusoidal wave and right BC* $u_x(0,t) = 0$.

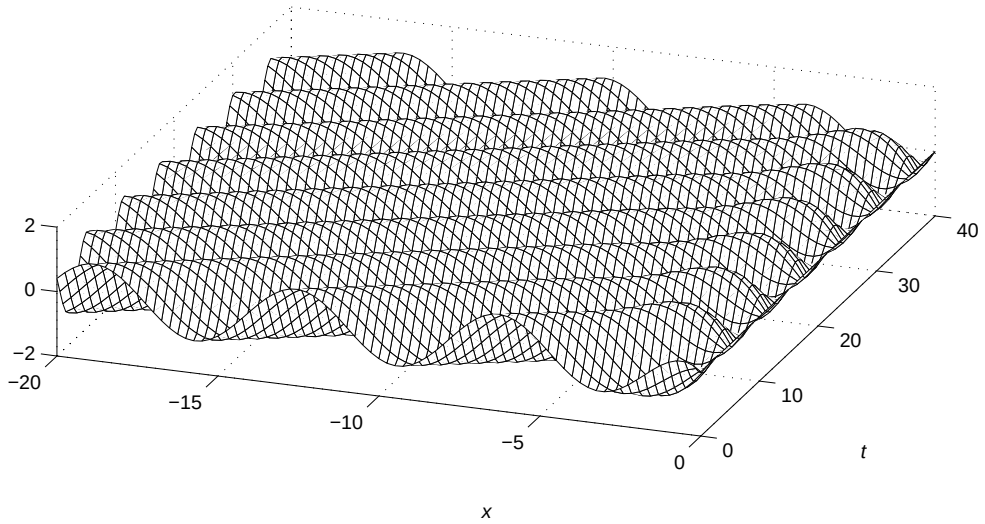

FIG. 3.6. *Solution to the left half-plane problem for* $u_t - u_{xxx} = 0$ *with incoming sinusoidal wave and right BC* $u(0,t) = 0$.

equation, we note that $\frac{u_n(x,t)}{t^n} = u_n(\xi)$ and $\frac{v_n(x,t)}{t^{n+1/3}} = v_n(\xi)$ both are functions of $\xi = \frac{x}{\sqrt[3]{t}}$ only, satisfying

$$(u_n)_{\xi\xi\xi} + \frac{\xi}{3}(u_n)_\xi - n\, u_n = 0, \;\; \{u_n(0) = 1,\ (u_n)_\xi(0) = 0,\ u_n(\infty) = 0\}$$

and

$$(v_n)_{\xi\xi\xi} + \frac{\xi}{3}(v_n)_\xi - (n + \tfrac{1}{3})\, v_n = 0, \;\; \{v_n(0) = 0,\ (v_n)_\xi(0) = 1,\ v_n(\infty) = 0\},$$

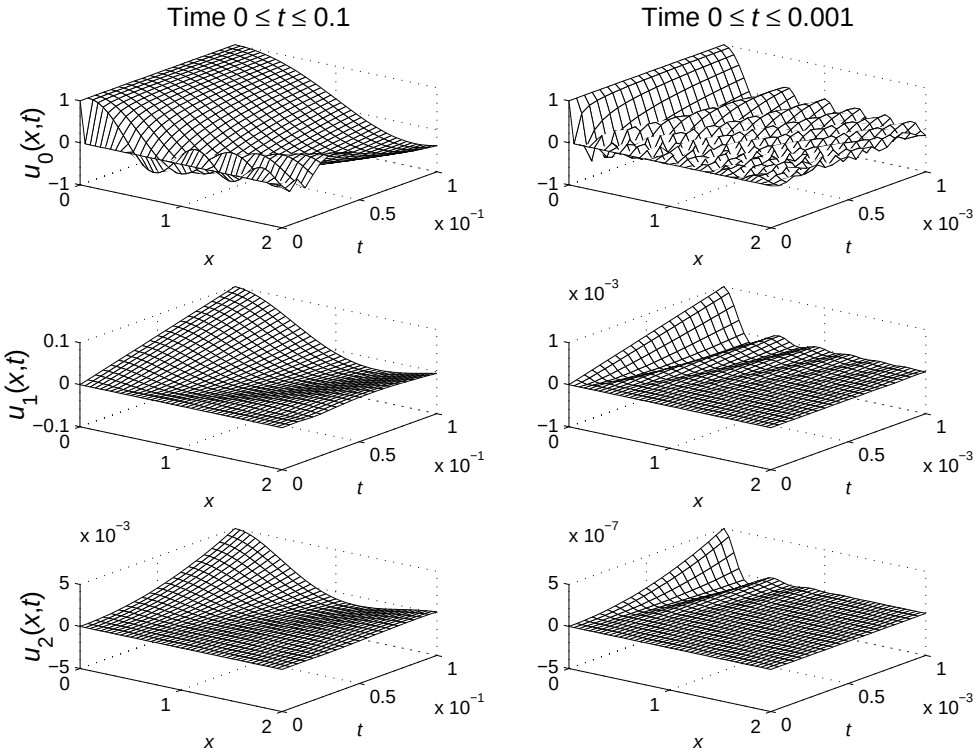

FIG. 3.7. *First three corner functions* $u_n(x,t)$ *for* $u_t - u_{xxx} = 0$, *displayed over* $0 \le t \le 0.1$ *and* $0 \le t \le 0.001$ *(left and right column, respectively).*

respectively, leading to the general expressions for the corner functions:

$$u_n(x,t) = t^n \left\{ {}_1F_2(-n, \{\tfrac{1}{3}, \tfrac{2}{3}\}, -\tfrac{x^3}{27t}) - \tfrac{x^2}{2t^{2/3}} \tfrac{\Gamma(n+1)}{\Gamma(n+\frac{1}{3})}\ {}_1F_2(\tfrac{2}{3} - n, \{\tfrac{4}{3}, \tfrac{5}{3}\}, -\tfrac{x^3}{27t}) \right\}, \quad n = 0, 1, 2, \dots,$$

and

$$v_n(x,t) = t^{n+\frac{1}{3}} \left\{ {}_1F_2(-n, \{\tfrac{2}{3}, \tfrac{4}{3}\}, -\tfrac{x^3}{27t}) - \tfrac{x^2}{2t^{2/3}} \tfrac{\Gamma(n+1)}{\Gamma(n+\frac{2}{3})}\ {}_1F_2(\tfrac{1}{3} - n, \{\tfrac{4}{3}, \tfrac{5}{3}\}, -\tfrac{x^3}{27t}) \right\}, \quad n = 0, 1, 2, \dots.$$

Figures 3.7 and 3.8 display the first three corner functions of each of the two types.

3.3. Right corner functions. Since the PDE is incapable of transporting any waves to the left, waves reaching a right side boundary will get absorbed no matter what BC is used there. As a consequence, the right corner functions on the domain $x < 0$, $t > 0$ will be nonoscillatory and reminiscent of the ones for the heat equation. Denoting these by $w_n(x,t)$, $n = 0, 1, 2, \dots$, we find by the same means as in the previous section

$$w_n(x,t) = t^n \left\{ {}_1F_2(-n, \{\tfrac{1}{3}, \tfrac{2}{3}\}, -\tfrac{x^3}{27t}) + \tfrac{x}{t^{1/3}} \tfrac{\Gamma(n+1)}{\Gamma(n+\frac{2}{3})}\ {}_1F_2(\tfrac{1}{3} - n, \{\tfrac{2}{3}, \tfrac{4}{3}\}, -\tfrac{x^3}{27t}) \right.$$
$$\left. + \tfrac{(-1)^n\sqrt{3}}{4\pi} \tfrac{x^2}{t^{2/3}} \Gamma(n+1)\ \Gamma(\tfrac{2}{3} - n)\ {}_1F_2(\tfrac{2}{3} - n, \{\tfrac{4}{3}, \tfrac{5}{3}\}, -\tfrac{x^3}{27t}) \right\},\ n = 0, 1, 2, \dots.$$

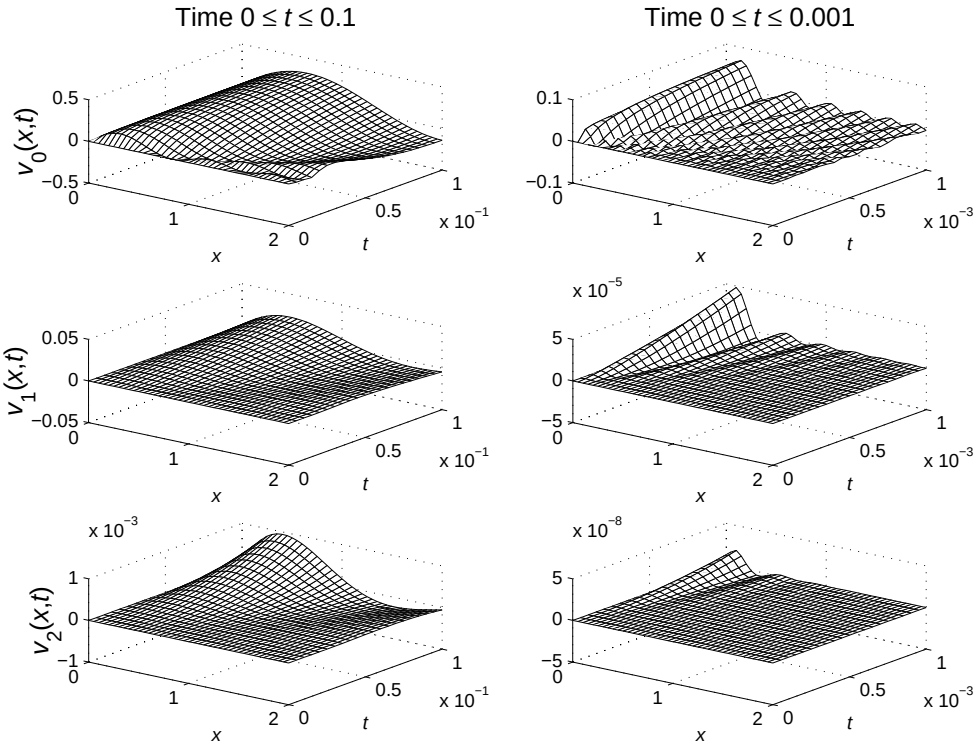

FIG. 3.8. *First three corner functions* $v_n(x,t)$ *for* $u_t - u_{xxx} = 0$, *displayed over* $0 \le t \le 0.1$ *and* $0 \le t \le 0.001$ *(left and right column, respectively).*

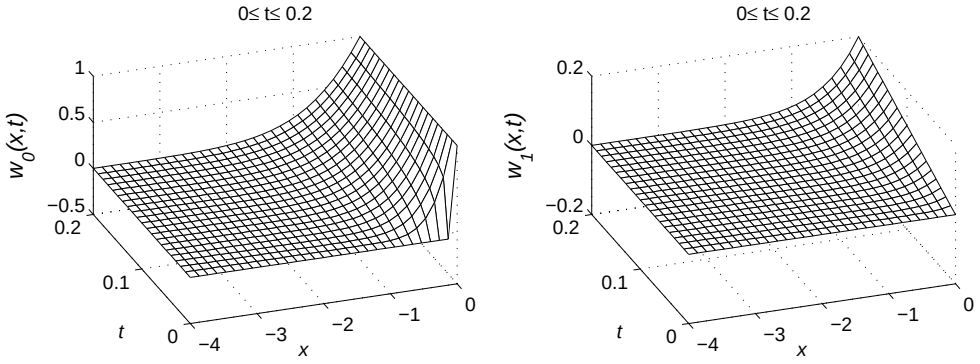

FIG. 3.9. *The right corner functions* $w_0(x,t)$ *and* $w_1(x,t)$ *to* $u_t - u_{xxx} = 0$.

Figure 3.9 displays the first two $w_n(x,t)$-functions.

For all the corner functions we have derived ($u_n(x,t)$ for the heat equation and $u_n(x,t)$, $v_n(x,t)$, $w_n(x,t)$ for the linearized KdV equation), the first hypergeometric function has $-n$ as its first parameter. This implies that, for $n = 0, 1, 2, \dots$, its usually infinite Taylor series truncates to become a finite degree polynomial.

To conclude this discussion of right corner functions, we note that a general

solution to (3.1) with

$$\begin{aligned} &\text{IC:} \quad u(x,0) = f(x), \quad x < 0, \\ &\text{BC:} \quad u(0,t) = g(t), \quad t > 0, \end{aligned}$$

can be expressed in terms of coupled contour principal value integrals [5].

4. Corner analysis for $iu_t - u_{xx} = 0$. The next example we consider is the linear Schrödinger equation

$$iu_t - u_{xx} = 0. \tag{4.1}$$

Although this also is a dispersive PDE, it will be shown that the character of IBV solutions for this equation is fundamentally different than for the linear KdV equation (3.1). Like the diffusion equation $u_t - u_{xx} = 0$, equation (4.1) requires only one BC on each side. Also, since the analysis is similar to that for the diffusion equation, we will here not consider any introductory half-plane problems.

4.1. Corner functions. Since $iu_t - u_{xx} = 0$ differs from the heat equation only by a factor of i, the same similarity transformation $\xi = \frac{x}{\sqrt{t}}$ and $\tau = \log t$ will again lead us to the corner functions. Substituting these transformations into $iu_t - u_{xx} = 0$ yields

$$iu_\tau - \frac{i\xi}{2} u_\xi - u_{\xi\xi} = 0. \tag{4.2}$$

The equilibrium solution satisfies

$$u_{\xi\xi} + \frac{i\xi}{2} u_\xi = 0,$$

leading to

$$u_0(x,t) = \operatorname{Erfc}\left(\sqrt{i}\frac{x}{2\sqrt{t}}\right) = \frac{1+i}{\sqrt{2\pi}} \int_{\frac{x}{\sqrt{t}}}^{\infty} e^{-i\frac{\eta^2}{4}} d\eta. \tag{4.3}$$

Separating (4.3) into real and imaginary parts results in

$$u_0(x,t) = 1 - S\left(\frac{x}{\sqrt{2\pi t}}\right) - C\left(\frac{x}{\sqrt{2\pi t}}\right) + i\left[S\left(\frac{x}{\sqrt{2\pi t}}\right) - C\left(\frac{x}{\sqrt{2\pi t}}\right)\right],$$

where S and C are the Fresnel sine, $\int_0^z \sin(\pi t^2/2)dt$, and cosine, $\int_0^z \cos(\pi t^2/2)dt$, functions. Higher-order corner functions are again most easily expressed in terms of hypergeometric functions. In analogy to (2.12), we obtain

$$u_n(x,t) = t^n \left\{ {}_1F_1(-n, \tfrac{1}{2}, \tfrac{-ix^2}{4t}) - \tfrac{x\sqrt{i}}{\sqrt{t}} \tfrac{\Gamma(n+1)}{\Gamma(n+\frac{1}{2})} {}_1F_1(\tfrac{1}{2} - n, \tfrac{3}{2}, \tfrac{-ix^2}{4t}) \right\}, \; n = 0, 1, \ldots,$$

which satisfies (4.1) with IC $u(x,0) = 0$ and the BCs $u(0,t) = t^n$, $u(\infty,t) = 0$.

The real and imaginary parts of the corner functions $u_0(x,t)$ and $u_1(x,t)$ are plotted in Figure 4.1.

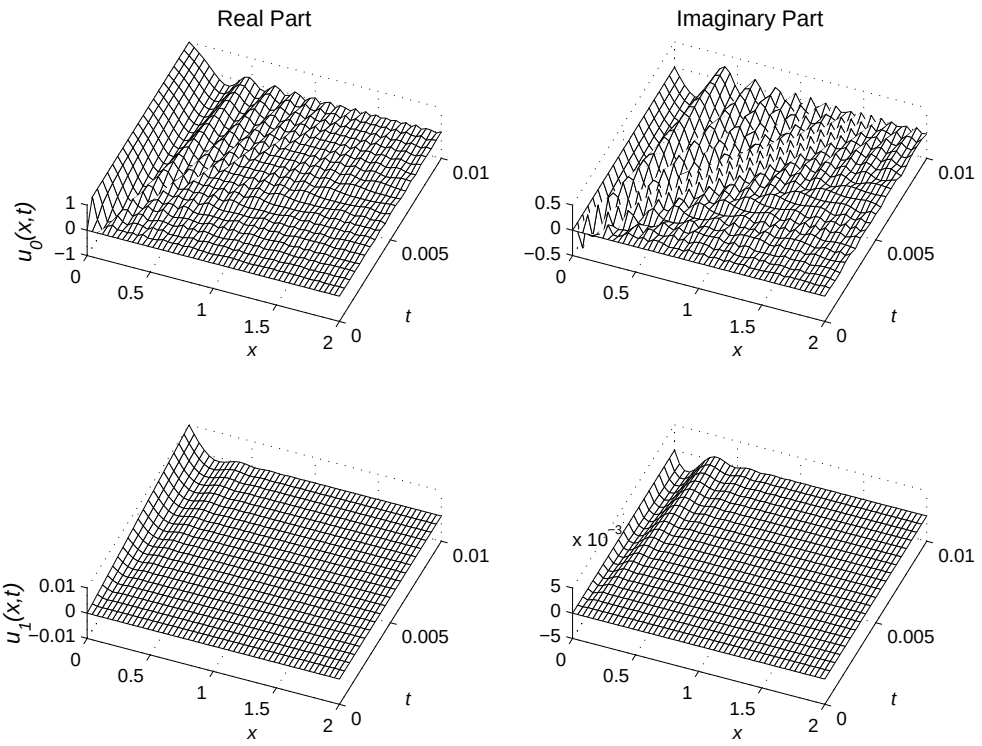

FIG. 4.1. *Real and imaginary part of the first two corner functions u_0 and u_1 to $iu_t - u_{xx} = 0$.*

5. Qualitative solution features in the case of two boundaries. In this section, the properties of $u_t - u_{xxx} = 0$ are contrasted with those of $iu_t - u_{xx} = 0$. In the former case ($u_t - u_{xxx} = 0$), high-frequency waves race across the interval and become absorbed at the opposite boundary. Like for the heat equation, the solutions are infinitely differentiable for all $t > 0$. In the latter case ($iu_t - u_{xx} = 0$), the waves are reflected off the boundaries for all times, resulting in a solution that is several times differentiable only for rare values of $t > 0$ (when recurrences to the IC happen to occur). This lack of smoothness has severe impact on the accuracy of straightforward numerical calculations.

5.1. Features of the solution to $u_t - u_{xxx} = 0$ in the case of two boundaries. Although the IBV problem

$$\begin{aligned} &\text{PDE:} && u_t - u_{xxx} = 0, && \\ &\text{IC:} && u(x,0) = 0, && 0 < x \le 1, \\ &\text{BCs:} && u(0,t) = f(t),\ u_x(0,t) = g(t),\ u(1,t) = 0, && t > 0, \end{aligned} \tag{5.1}$$

does not appear to admit a simple closed form solution for general functions $f(t)$ and $g(t)$, it can be verified that the function

$$u(x,t) = \frac{3}{2\pi} \int_0^\infty \frac{e^{\frac{1}{2}rx - r^3 t}}{r} \sin\left(\frac{\sqrt{3}}{2} r(x-1)\right) \left(e^{-3r/2} + 2\cos\left(\frac{\sqrt{3}}{2} r\right)\right) dr \tag{5.2}$$

satisfies it for some particular choice of $f(t)$ and $g(t)$. We note the following:

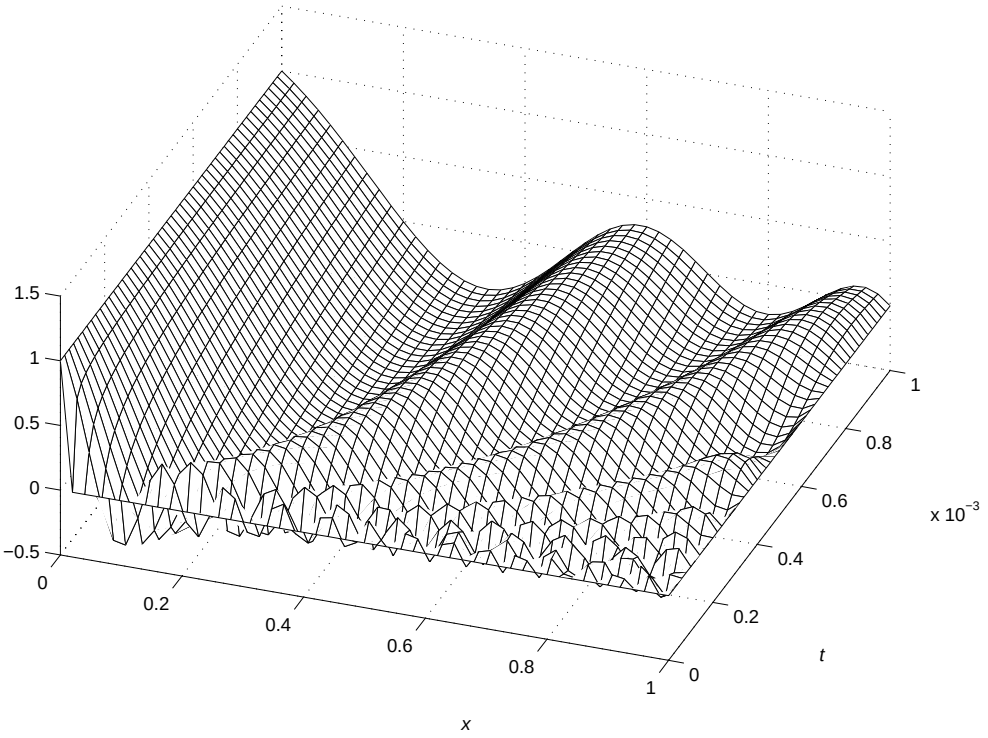

FIG. 5.1. *Solution* $u(x,t)$ (5.2) *to the IBV problem for* $u_t - u_{xxx} = 0$, *displayed for time* $0 \le t \le 10^{-3}$.

- $\lim_{t\to 0+} u(x,t) = 0$ for $0 < x \le 1$ (although the integral for $u(x,t)$ diverges if $t = 0$ is substituted directly into it).
- The function $f(t)$ (as obtained from (5.2)) is not identically equal to one although it satisfies $f(0) = 1$ and $f^k(0) = 0,\ k = 1, 2, \ldots$.

Figure 5.1 shows $u(x,t)$ for $0 \le t \le 10^{-3}$, illustrating how high-frequency waves emerge out of the singular corner and then get absorbed (with no reflections) at the right edge.

5.2. Features of the solution to $iu_t - u_{xx} = 0$ in the case of two boundaries. Consider the IBV problem

$$\begin{aligned} &\text{PDE:} && iu_t - u_{xx} = 0, && \\ &\text{IC:} && u(x,0) = 0, && 0 \le x \le 1, \\ &\text{BCs:} && u(0,t) = \sin t,\ u(1,t) = 0, && t > 0. \end{aligned} \tag{5.3}$$

The long-term solution

$$u_L(x,t) = \frac{i}{2}\left(e^{it}\frac{\sin(1-x)}{\sin 1} - e^{-it}\frac{\sinh(1-x)}{\sinh 1}\right)$$

satisfies the PDE and the BCs. The fast scale solution, emanating from the corner, is

$$u_T(x,t) = u(x,t) - u_L\,(x,t)$$

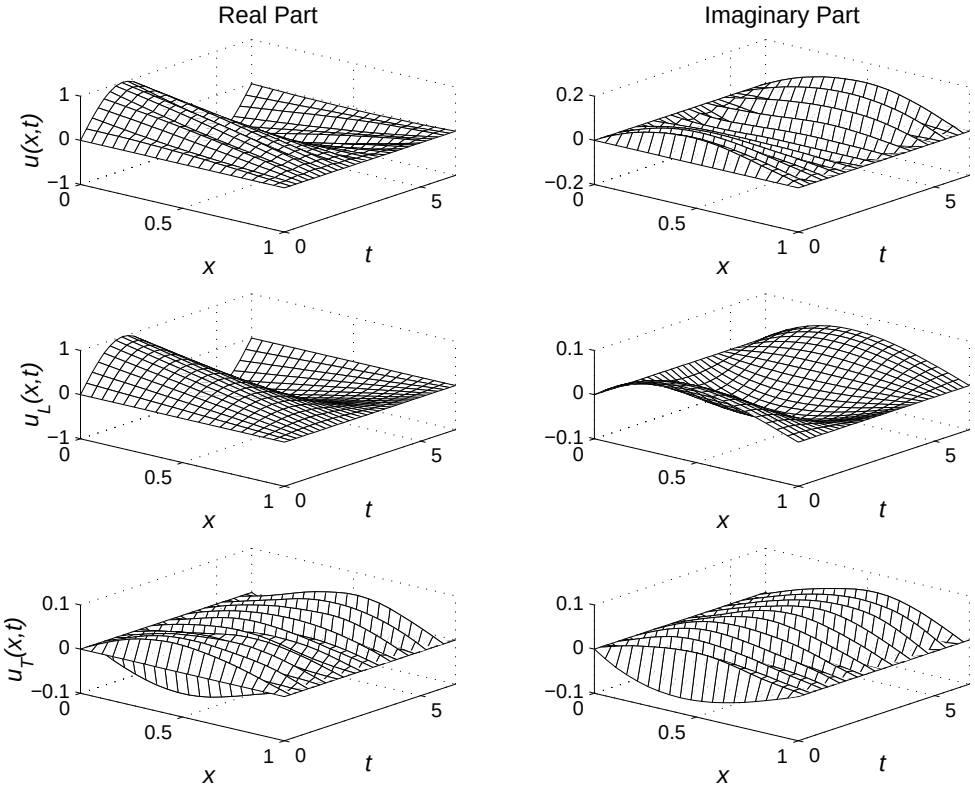

FIG. 5.2. *Full solution $u(x,t)$, long-term solution $u_L(x,t)$, and transient solution $u_T(x,t)$ for* (5.3).

and will again need to satisfy the PDE but with different IC and BC:

$$\begin{aligned} &\text{IC:} \quad u_T(x,0) = -\tfrac{i}{2}\left(\tfrac{\sin(1-x)}{\sin 1} - \tfrac{\sinh(1-x)}{\sinh 1}\right), && 0 \le x \le 1, \\ &\text{BC:} \ u_T(0,t) = u_T(1,t) = 0, && t > 0. \end{aligned}$$

It can be written as a simple sine series expansion:

$$u_T(x,t) = 2\pi i \sum_{k=1}^{\infty} \frac{k}{1-(k\pi)^4} e^{i(k\pi)^2 t} \sin k\pi x. \tag{5.4}$$

Figure 5.2 shows the real and imaginary parts of the $u(x,t)$, $u_L(x,t)$, and $u_T(x,t)$. Figure 5.3 shows the full solution over a short time interval, revealing

1. emanating waves from the corner, as described by the $u_n(x,t)$ corner functions (cf. Figure 4.1) and
2. the reflection of all waves at the boundaries.

The latter fact means that, in contrast to the heat equation, $u_t - u_{xx} = 0$, or the linear KdV equation, $u_t - u_{xxx} = 0$, the solution will not become smoother with time. Indeed, (5.4) shows that $\frac{\partial^4 u}{\partial x^4}$ and $\frac{\partial^2 u}{\partial t^2}$ will fail to exist at almost all x and t. Unless (5.3) is modified to contain some form of dissipation (interior or at the boundaries), accurate numerical solutions would appear to be quite difficult to obtain.

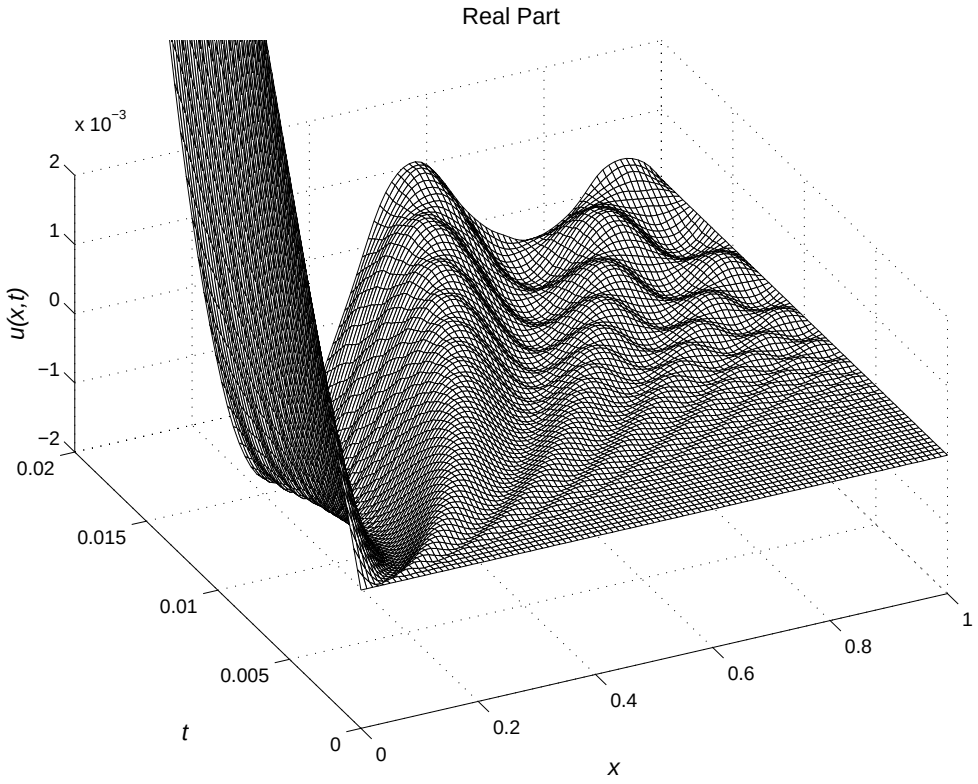

FIG. 5.3. *Real part of the solution $u(x,t)$ to the IBVP test problem for $iu_t - u_{xx} = 0$, shown for $0 \le t \le 0.02$.*

6. Concluding remarks. Since the initial data and the boundary data for PDEs typically arise from different considerations, discrepancies will almost always occur in the corners of the time-space domain. Unless infinitely many compatibility conditions hold in the corners, the solutions will feature singularities which may or may not remain local in time and space. With modern high-order or spectral methods, these discrepancies are often the dominant source of numerical error. It is thus essential to

1. identify and understand the nature of the corner singularities for the IBV problem being solved, and
2. devise numerical remedies to restore expected levels of accuracy.

Both issues have been addressed for second-order convective-diffusive equations in [4]. This study has focused on the first point above for dispersive equations, showing that the concept of corner basis functions, introduced in [4], is critical in understanding the nature of the singularities.

To summarize the different characters of the corner singularities for the PDEs considered, analytic expressions for the first corner basis function, $u_0(x,t)$, are given in Table 6.1 and are graphically contrasted over two different time intervals in Figure 6.1. The analytical form of the corner basis functions for the general PDE $u_t \pm u_{nx} = 0$, $n = 1, 2, 3, \ldots$, has also been included in the table. The constants c_k are determined by the BC $u_0(0,t) = 1$ and all higher derivative BCs equal to zero. The dissipative case $u_t - u_{4x} = 0$ is also illustrated.

TABLE 6.1
Analytic expressions for the $u_0(x,t)$ corner functions for some PDEs of the form $u_t \pm u_{nx} = 0$.

Equation	Elementary form	Hypergeometric form
$u_t - u_x = 0$	0 if $x > t$ 1 if $x < t$	—
$u_t - u_{xx} = 0$	$\operatorname{Erfc}\left(\frac{x}{2\sqrt{t}}\right)$	$1 - \frac{x}{\sqrt{\pi t}}\ {}_1F_1\left(\frac{1}{2}, \frac{3}{2}, -\frac{x^2}{4t}\right)$
$u_t - u_{xxx} = 0$	—	$1 - \frac{\sqrt{3}\,\Gamma(\frac{2}{3})\,x^2}{4\pi\, t^{2/3}}\ {}_1F_2\left(\frac{2}{3}, \left\{\frac{4}{3}, \frac{5}{3}\right\}, -\frac{x^3}{27t}\right)$
$u_t + u_{4x} = 0$	—	$1 - \frac{1}{2\sqrt{\pi}}\frac{x^2}{t^{2/4}}\ {}_1F_3\left(\frac{2}{4}, \left\{\frac{3}{4}, \frac{5}{4}, \frac{6}{4}\right\}, \frac{x^4}{256t}\right)$ $+\frac{\Gamma(\frac{3}{4})}{6\pi}\frac{x^3}{t^{3/4}}\ {}_1F_3\left(\frac{3}{4}, \left\{\frac{5}{4}, \frac{6}{4}, \frac{7}{4}\right\}, \frac{x^4}{256t}\right)$
$\vdots$	$\vdots$	$\vdots$
$u_t \pm u_{nx} = 0$	—	$\sum_{k=0}^{n-1}\left[c_k \frac{x^k}{t^{k/n}}\right.$ $\left.\times\ {}_1F_{n-1}\left(\frac{k}{n}, \left\{\frac{k+1}{n}, \frac{k+2}{n}, \dots, \frac{k+n}{n}\right\}, \pm\frac{x^n/t}{n^n}\right)\right]$, where the c_k are constants; the entry $= 1$ is omitted in the sequence $\left\{\frac{k+1}{n}, \frac{k+2}{n}, \dots, \frac{k+n}{n}\right\}$

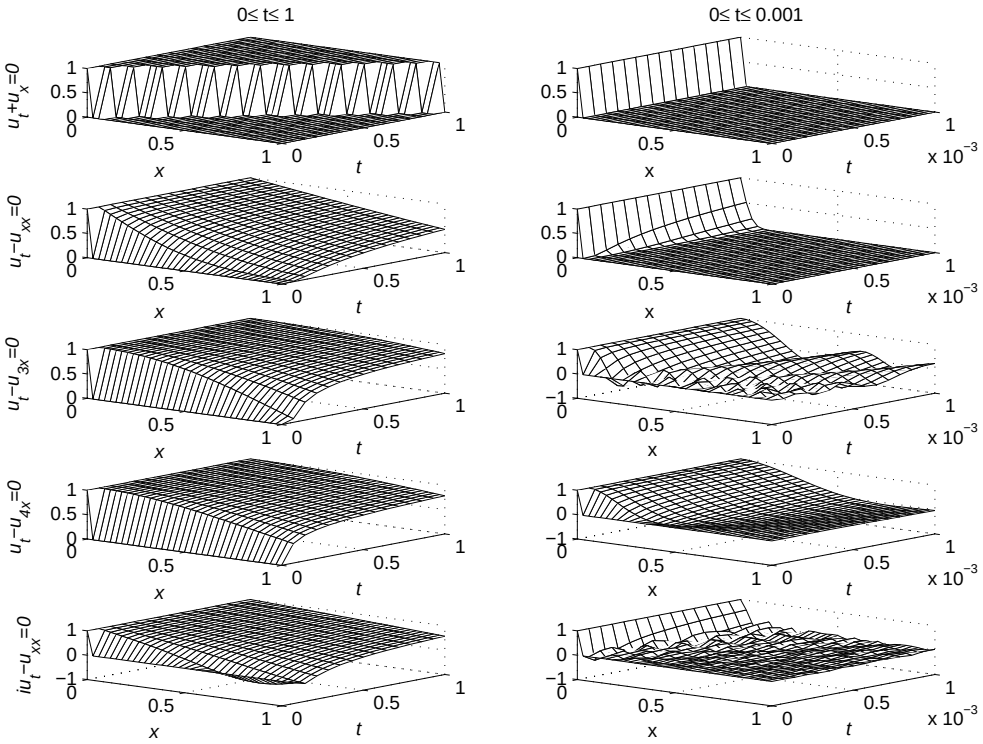

FIG. 6.1. *The $u_0(x,t)$ corner functions for the equations, $u_t \pm u_{nx} = 0$, $n = 1, \dots, 4$, and $iu_t - u_{xx} = 0$ (real part).*

The nature of the corner singularities for each PDE is different, including propagation of the discontinuity throughout the domain, dissipation of it locally, and high-frequency oscillations which either get absorbed or reflected at boundaries. In subsequent studies, numerical techniques for restoring accuracy of high-order and spectral methods for dispersive IBV problems will be explored.

REFERENCES

[1] E.W. Barnes, *The asymptotic expansion of integral functions defined by generalized hypergeometric series*, Proc. London Math. Soc. Ser. 2, 5 (1906), pp. 59–116.

[2] J.P. Boyd and N. Flyer, *Compatibility conditions for time-dependent partial differential equations and the rate of convergence of Chebyshev and Fourier spectral methods*, Comput. Methods Appl. Mech. Engrg., 175 (1999) pp. 281–309.

[3] N. Flyer and P.N. Swarztrauber, *The convergence of spectral and finite difference methods for initial-boundary value problems*, SIAM J. Sci. Comput., 23 (2002), pp. 1731–1751.

[4] N. Flyer and B. Fornberg, *Accurate numerical resolution of transients in initial-boundary value problems for the heat equation*, J. Comput. Phys, 184 (2003), pp. 526–539.

[5] A. Fokas and B. Pelloni, *The solution of certain initial boundary-value problems for the linearized Korteweg-deVries equation*, R. Soc. Lond. Proc. Ser. A Math. Phys. Eng. Sci., 454 (1998), pp. 645–657.

[6] B. Fornberg, *A Practical Guide to Pseudospectral Methods*, Cambridge Monogr. Appl. Comput. Math. 1, Cambridge University Press, Cambridge, UK, 1996.